Fuel 123 (2014) 218–229

Contents lists available at ScienceDirect

Fuel

journal homepage: www.elsevier.com/locate/fuel

Study on the spray and combustion characteristics of water–emulsified diesel

Ming Huo [a], Shenlun Lin [b,c], Haifeng Liu [d], Chia-fon F. Lee [a,e,*]

[a] Department of Mechanical Science and Engineering, University of Illinois at Urbana-Champaign, IL 61801, USA
[b] Center of General Education, Cheng Shiu University, Kaohsiung 83347, Taiwan
[c] Super Micro Mass Research and Technology Center, Cheng Shiu University, Kaohsiung 83347, Taiwan
[d] State Key Laboratory of Engines, Tianjin University, Tianjin 300072, China
[e] Center for Combustion Energy and State Key Laboratory of Automotive Safety and Energy, Tsinghua University, Beijing 100084, China

HIGHLIGHTS

- HLB = 5 is the most suitable surfactant composition for emulsified diesel.
- Puffing and disruptive droplet combustion observed near flame lift-off.
- Identify the potential micro-explosion impact on primary breakup.
- Measure the emulsified diesel liquid penetration under various ambient conditions.

GRAPHICAL ABSTRACT

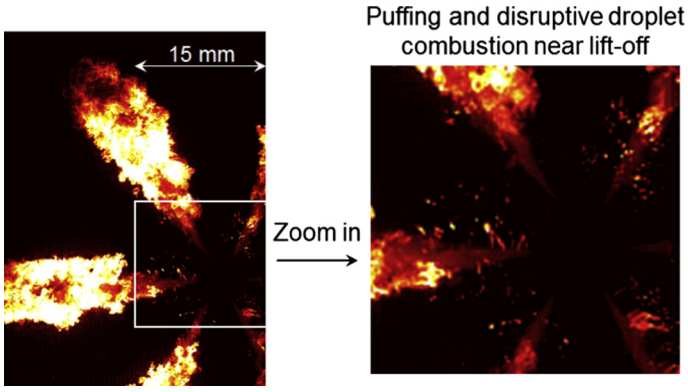

ARTICLE INFO

Article history:
Received 27 September 2013
Received in revised form 10 December 2013
Accepted 14 December 2013
Available online 7 January 2014

Keywords:
Water emulsified fuel
Micro-explosion
Spray
Combustion

ABSTRACT

Emulsified fuel remains a potential solution to meet the increasingly stringent emission regulations for internal combustion engines due to its capability of simultaneously reducing NO_x and particular matter (PM). In this study, emulsified diesels with 10% and 20% water by volume were studied. The stability of the water emulsified diesel was first investigated in terms of the hydrophilic-lipophilic-balance (HLB) value. Based on the stability test, a suitable surfactant composition for the diesel/water interfacial condition was given and the separation tendency of the fuel with different water volumetric ratio was analyzed. The emulsions were later injected and combusted in a pre-burn type constant volume chamber, which is able to provide high ambient temperature and pressure to mimic real engine operation conditions. High speed imaging was used to capture the spray and combustion process under various conditions. Results show longer initial liquid penetration for emulsified diesel under low ambient temperatures. Longer ignition delay of emulsified diesel also provided more air/fuel mixing time, thus significantly lowering the soot luminosity.

Although droplet micro-explosion has been intensively studied, its behavior in a burning spray is much less reported. This study in particular focused on micro-explosion in a burning spray. Broadband natural flame images were recorded with intentional overall over-exposure such that the central lift-off region could be illuminated by soot incandescence. Puffing and disruptive droplet combustion was consistently observed at high ambient temperature in the central lift-off region with emulsified diesel indicating the occurrence of micro-explosion in a burning spray flame. It is demonstrated that micro-explosion is not

* Corresponding author at: Department of Mechanical Science and Engineering, University of Illinois at Urbana-Champaign, IL 61801, USA. Tel.: +1 217 3335879; fax: +1 217 2446534.
E-mail address: cflee@illinois.edu (C.F. Lee).

http://dx.doi.org/10.1016/j.fuel.2013.12.035

only able to enhance the secondary breakup, but also affect the primary breakup under certain conditions, which to the author's awareness has not been reported in any previous literature. Lower injection pressure and higher ambient temperature favor the occurrence of micro-explosion before primary breakup as a competition between the micro explosion delay time and the primary breakup time.

1. Introduction

Many alternative fuels for diesel engines have been investigated and developed driven by the increasingly stringent emission regulations as well as the depletion of fossil fuels. Fuel emulsification, a potential solution to the "Particulate Matter (PM)-NO_x trade-off", has received much attention in the last two decades [1–6].

Emulsified fuel's capability of reducing NO_x can be attributed to the vaporization of water, which suppresses the local adiabatic flame temperature and thus notably reduces the NO_x emissions. Its soot reduction capability can be explained by the better air fuel mixing process featured by enhanced atomization since micro-explosion may occur due to the drastic volatility difference between the different phases of the fuel. Moreover, water dissociation can form hydroxyl radicals during combustion which help to oxidize the soot thus reducing soot emissions [5]. The micro-explosion phenomenon, which greatly enhances fuel atomization, is of particular interest in academia. In the combustion of a multi-component droplet with its components possessing vastly different volatilities, a micro-explosion event will be induced by the superheating of the more volatile components that are trapped in the interior of the droplet whose overall boiling temperature is controlled by the less volatile component in the mixture. The occurrence of such an event causes violent secondary breakup and as such, the burning rate of the droplet is significant increased [7]. Although the existence of micro-explosion for a single fuel droplet has been well documented [7–15], the presence of such phenomena in either a combusting or non-combusting spray and how it facilitates atomization is still open to question. The observation of micro-explosion in droplet combustion arouses interest in finding similar evidence in a real engine combustion environment. Note that droplet behaviors as well as the ambient conditions in a spray are substantially different from those conducted in single droplet experiments. Therefore, the hypothesis that micro-explosion occurs in a spray and helps enhance the secondary breakup which ultimately reduces the soot and NO_x emission still requires further experimental support. The injection and ambient conditions that potentially favor the occurrence of micro explosion in spray combustion also need to be explored.

The presence of micro-explosion in atomized emulsion sprays were demonstrated in separate experiments by a number of investigators [16,18–25]. For the non-combusting spray, Mattiello et al. [16] studied the water/fuel–oil emulsion flames by laser light scattering, the analysis of the scattered light intensities of the polarization ratio supported the occurrence of micro-explosion in the flame. Wu et al. [17] used laser holography shadowgraph to visualize the spray in a diesel/water/ethanol emulsion in which an apparent raised part could be seen in the main jet body which suggested the occurrence of micro-explosion. Watanabe and Okazaki [18] used extremely high speed imaging to visualize the secondary atomization in an emulsified-fuel spray flow by shadow imaging; they reported puffing and partial-micro-explosion, but complete micro-explosion was rarely observed. For the combusting spray, the direct flame photographs, temperature profiles and micro-explosion frequencies have been shown by Fuchihata et al. [19–21]. They reported observation of small droplets with diameters less than 50 μm exploding in the spray flame. In the study of Raul et al. [22], some "glowing spots" were observed inside the burning spray and might have resulted from micro-explosion. A summary of the visual evidence of micro-explosion in previous studies has been listed in Table 1. To date, observations such as increased cone angle, unusual jet body detachment on the tip/periphery of the spray, glowing spots are often used as evidence of micro-explosion whereas direct visualization were much less reported. The challenge of capturing the phenomena not only comes from the demanding hardware requirement for high temporal and spatial resolution, but also from the nature of the phenomenon itself, as micro-explosion is a highly transient process and is very sensitive to the fuel properties as well as ambient conditions. In the single droplet tests [15], it has been illustrated that micro-explosion can occur over a broad range of temperatures and waiting times and its occurrence is statistically based. It is therefore reasonable to assume a similar scenario for micro-explosion in a spray flame. All these factors make the capture of micro-explosion in a spray very challenging.

The primary motivation of the present study is to explore micro-explosion in a spray flame by investigating the spray and combustion characteristics of emulsified diesel under a wide range of conditions. High speed (15037 frames/s) liquid scattering imaging and broad-band luminosity imaging were carried out for studying the spray and combustion process respectively. The impact of ambient temperature and injection pressure on the spray penetration and natural luminosity were evaluated for emulsified diesel with different blending ratios. By intentional overall over-exposure of the natural flame imaging, puffing and disruptive droplet combustion were observed in a burning spray flame around the lift-off region, which to the author's knowledge has never been reported before. The experimental data will also be of great value in future micro-explosion modeling in a burning spray. A secondary motivation of the study is to address the stability issue of emulsified diesel in view of the hydrophilic-lipophilic-balance (HLB) value. The HLB value of a surfactant is a measure of the degree to which it is hydrophilic or lipophilic, which is defined as: $HLB = 20 \times M_h/M$, where M_h is the molecular mass of the hydrophilic portion of the molecule. It is based on a scale of 0–20 where a value of 20 corresponds to a completely hydrophilic molecule. A suitable surfactant composition for the diesel/water interfacial condition will be given based on the stability test. The separation tendency of the fuel with different water volumetric ratios is also analyzed providing guidance in future diesel-emulsion preparations.

2. Experimental method

2.1. Preparation of emulsified fuel

Ultra low sulfur diesel (ULSD) was used as the base fuel and the oil phase in the current study, with its properties tabulated in Table 2. A hydrophilic surfactant TWEEN 80 with an HLB value of 15 was added into water for reducing the interfacial tension and retarding the flocculation, coalescence, and creaming between oil and water phases. Meanwhile, Span 80 with an HLB value of 4.3 was added into ULSD to stabilize the oil phase. A magnetic stirrer

Table 1
Summary of previous works on micro-explosion in a spray.

Ref.	Fuel	Ambient temperature (K)	Observations
Mattiello et al. [16]	Oil with 0%, 10% and 20% by weight of emulsified water	–	Difference in the scattered light intensity and polarization ratio
Wu et al. [17]	Diesel water methanol emulsions	773	Raised part from the main jet body
Watanabe and Okazaki [18]	Dodecane and water	823	Direct visualization of droplet puffing in the secondary breakup
Fuchihata et al. [19–21]	Light oil–water emulsified fuel 70% light oil, 28% water, 2% surfactant	-	Blurring image on a series of sequential images
Raul et al. [22]	Macro-emulsion with 88% diesel, 10% water and 2% additive; Micro-emulsion with 80% diesel, 10% water and 10% additive	830 K	Glowing spots in the flame
Park et al. [23]	88% Diesel, 10% water, 2% additive	–	Group of droplets inside luminous flames
Lin and Lin [24]	Micro-emulsion with 80% diesel, 10% water, and 10% additive (surfactants)	653	Enhanced spray angle
Sheng et al. [25]	10%, 12% Water diesel emulsion	733–823	Ejection of fragments of torn droplets expanding the spray head and cone angle
Liu et al. [26]	Butanol–biodiesel, ethanol–biodiesel blends	800–900	Erupted spray jet and expanded spray tip

(Temper, Fisher Scientific Inc.) was employed to mix and heat the water and ULSD while the TWEEN 80 and Span 80 were added in respectively. A two-step procedure, similar to the one in Ref. [6], was utilized to prepare the oil-in-water-in-oil (O/W/O) emulsions in this research: an oil-in-water (O/W) emulsion was first prepared by adding 1/9 by volume USLD into water-TWEEN 80 mixture and blended at 10,000 RPM for 5 min. The above mixture was then gently poured into the ULSD-Span 80 mixture and emulsified for a period of time at 50 °C and 10,000 RPM to form O/W/O emulsion. In the final product, the water contents varied from 5 to 20 vol.% with fixed 2 vol.% total surfactant ratio. In the rest of the text, the ULSD emulsions will be represented by *W* + number with number indicating the volumetric ratio of the water.

The HLB value is the most referable parameter of surfactant selection in the emulsification process as higher HLB value can be interpreted as higher hydrophilic tendency of a surfactant. In the mixture, combined HLBs were used and calculated by the following equation:

$$HLB_{comb} = HLB_S \times W_S + HLB_T \times W_T \quad (1)$$

where subscripts *S* and *T* stands for Span 80 and TWEEN 80 respectively; *W* is the mass ratio of each surfactant ($W_S + W_T = 1$). In order to optimize each surfactant volumetric ratio with respect to the fuel stability, W20 emulsions with HLB_{comb} value varied from 5.0 to 8.0 were tested and the stability results indicated that $HLB = 5$ is relatively the most suitable surfactant composition for the diesel/water interfacial condition.

The following two methods were employed to characterize the stability of the emulsion: (1) a two-week (14-day) continuous record of daily fuel changes; and (2) observation and analysis of dispersed water bubble sizes in the compound using an optical microscope (OLYMPUS BX51TF, TOKYO, JAPAN) with 400× amplification coupled with a CCD camera. The first method is aimed at observing the destabilization tendency of the emulsion after short term storage. Each tested fuel was stored in a centrifugal tube at an ambient temperature of 25 °C immediately after their production. A larger separated water phase volume at the bottom of tube towards the end of the 14-day standing means lower stability of the emulsion. In order to estimate the phase separation tendency after a long-term storage, the second method was carried out to capture the micro images of the water bubbles. The Sauter mean diameter (SMD) distribution of the water bubbles was further obtained using the image post-processing software (Image-Pro Plus). With the water bubble size distribution and SMD measurement, the tendency of phase separation could be predicted.

Table 2
Base line fuel properties.

Molecular formula	C_{12}–C_{25}
Cetane index	40 (min)
Total sulfur (ppm)	7–15
Density (g/ml)	0.82–0.86
Auto-ignition temperature (°C)	~210
Lower heating value (MJ/kg)	42.5
Flash point (°C)	65–88
Boiling point (°C)	180–230
90% Distillation point (°C)	293.3–332.2
Viscosity (cst)	1.5–4.5

2.2. Experimental setup and procedure

A constant volume chamber with a bore of 110 mm and a height of 65 mm was used in this study. The chamber could mimic the real diesel engine environment by burning a pre-mixture of acetylene, oxygen and nitrogen. A hydraulic-actuated electronic-controlled unit injector (HEUI) was mounted at the center of the chamber head, and its configurations are tabulated in Table 3. After the burning of the mixture, the chamber's ambient environment contained 21% oxygen, 66.7% nitrogen, 8.2% carbon dioxide and 4.1% water vapor by volume. The molecular weight for the post-combustion gas mixture was 29.74 kg/kmole, and the density was 14.8 kg/m^3. The ambient temperatures upon the injection ranged from 800 K to 1200 K, covering both low-temperature combustion and conventional combustion in diesel engines. Detailed experimental setup and procedure can be found in Ref. [26–28].

2.3. Optics

High speed imaging for both spray and combustion studies was carried out using a non-intensified high speed digital camera (Phantom V7.1). For the spray studies, the light source was supplied by a copper vapor laser (Oxford Lasers LS20-50) which can be externally controlled to run up to a maximum frequency of 50 kHz with pulse duration of 25 ns. The high-speed camera and the copper-vapor laser were synchronized to 15,037 frames per second with an exposure time of 3 μs to produce time resolved measurements at a spatial resolution of 512 × 256 pixels. The copper-vapor laser has two-color output, at 511 and 578 nm, with a power ratio of 2:1. To filter out the light at 578 nm for this monochromatic light extinction, two interference filters at 510 nm and 515 nm with 10 nm full width at half maximum (FWHM) achieving a 5 nm FWHM were mounted in front of the camera. The scattered light signal from the spray was received by a Nikkor lens with 105 mm focal lens. The camera was triggered by the injection

Table 3
Injector parameters.

Nozzle type	Valve-covered orifice
Number of nozzle holes	6
Orifice diameter	0.145 mm
Injection duration	3.5 ms
Fuel temperature	350 K

signal and was set to record for a sufficiently long duration to cover the entire spray and combustion event. The spatial resolution of the camera was typically 0.108 mm/pixel. The continuous-wave laser beam was expanded to completely illuminate the liquid spray as shown in Fig. 1. This "volume-illumination" method, rather than a laser sheet, was utilized to ensure that all droplets spreading from the nozzle were illuminated to identify the maximum axial and radial distances of any liquid-phase fuel. The input beam was directed at a slight angle to avoid interference with the camera.

For spray image post-processing, the raw images obtained from each complete injection sequence were first corrected by the first ten images of the respective sequence which were taken right before fuel injection. The histogram equalization was then performed to enhance the contrast of each image and minimize the effect of the illumination intensity variation due to the ambient temperature differences and light degradation from case to case. The liquid penetration was determined from a pre-determined threshold. It is worthwhile to mention that the penetration was not merely decided by "one" pixel reaching the threshold, but rather a 3×3 pixel arrays whose values were all above the threshold such that the possibility of detecting a false penetration tip could be reduced. All the quantitative analyses were averaged over at least five shots for a statistical basis.

As for the combustion study, two different camera configurations were used for different purposes as shown in Fig. 2. In the first configuration (the same configuration as in Mie scattering, thus exactly the same field of view), the camera resolution was 512×216 with a speed of 15037 fps. A relative larger camera aperture size of *f*/22 with intentional over-exposure was chosen such that stronger signal at lift-off region could be captured. The essence of this imaging method is that the strong chemical luminosity and soot incandescence from the diffusion flame could also illuminate the liquid phase in the flame lift-off region. In a typical broad-band natural flame luminosity measurement, over-exposure should be by all means avoided due to (1) over-exposure could cause image saturation downstream of the flame thus causing loss of information and (2) the signal from liquid scattering may contribute to the total "natural luminosity" causing ambiguity in the post-processing. However, we found that the over-exposure was an effective way for liquid illumination especially at the downstream central region of the lift-off for micro-explosion detection purposes; therefore two different camera configurations were applied. In the second configuration, the camera resolution of 640×480 and a frame rate of 8082 fps were used for the integrated broadband luminosity measurement. A minimum aperture size of *f*/32 on the lens was used to ensure no pixel saturation occurred downstream of the image.

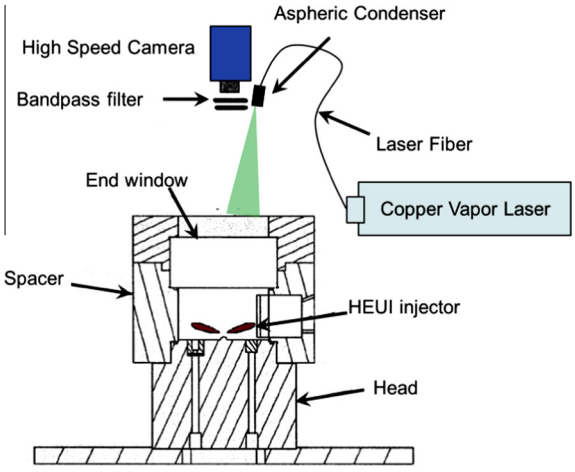

Fig. 1. Schematic of test rig.

3. Results and discussion

3.1. Fuel stability

After a 14-day standing, separate layers were clearly observed in W20 emulsions with HLB equal to 6, 7, and 8, while only HLB value of 5 presented a milky-white emulsion with no separate layers indicating that this was the suitable surfactant composition for the diesel/water interfacial condition. However, neither blending duration time nor water content showed any significant impact on the appearance of the emulsions, as all of them displayed one stable crystalline phase. Thus, micro-scale observation was further carried out to evaluate the phase separation tendency after a 14-day standing.

The dispersed water bubble size distribution and SMD are usually used to grade the homogeneities of different fuels. Additionally, a smaller droplet diameter leads to greater reaction surface per volume of fuel, thus promoting more complete combustion. Fig. 3 demonstrates the water bubble appearances, sizes and homogeneities of W5, W10, W15 and W20 under a 400× microscope after a 14-day standing. It can be seen that W5 has the smallest and most homogeneous dispersed water bubble distribution while the number of big bubbles increases with the water content. For the quantitative analysis, Fig. 4 illustrates the probability density function (PDF) of the O/W/O bubble sizes. The PDF curves displayed that W5 and W10 had relatively higher fractions of small bubbles around 2 μm while W15 and W20 had lower peak value at the smaller diameter region. Additionally, W10, W15 and W20 had an extra peak close to 4 μm which implies a more non-homogeneous distribution relative to W5. The volumetric density

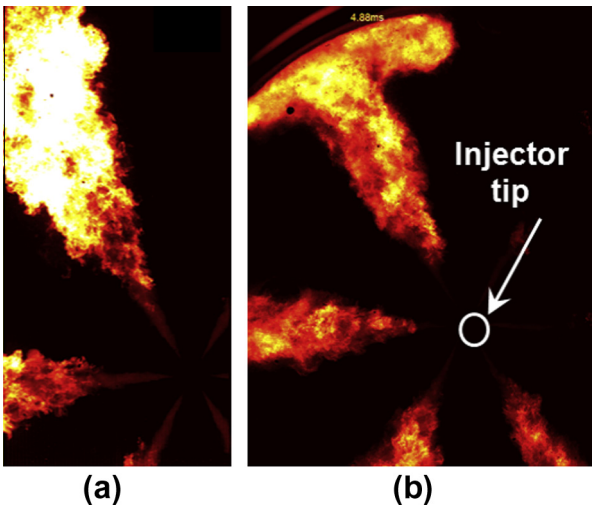

Fig. 2. Broadband luminosity images (a) 512×216 resolution, 15037 fps, camera aperture f/22 and (b) 640×480 resolution, 8082 fps, camera aperture f/32, the images are from two different spray events.

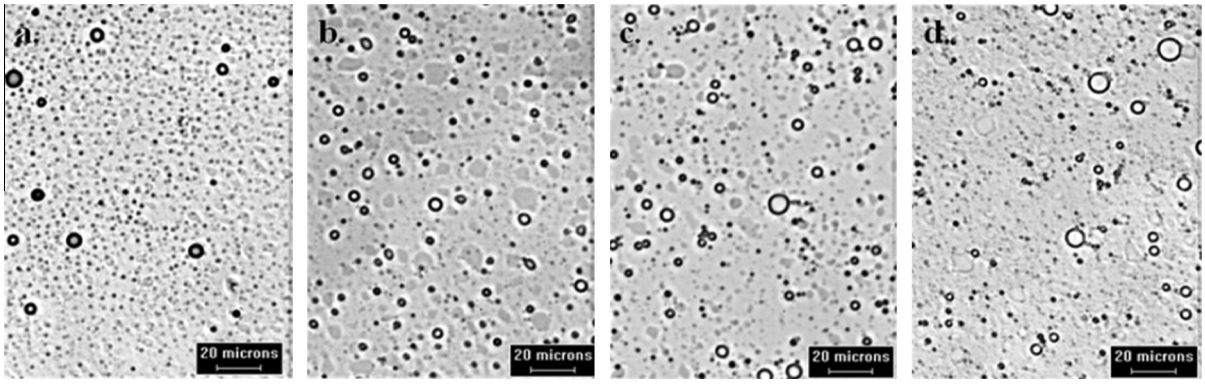

Fig. 3. O/W/O bubbles of water-diesel emulsion with (a) 5%; (b) 10%; (c) 15%; and (d) 20% water contents under 400× microscope.

function (VDF) was defined as: (the volume ratio of water bubble with specific diameter)/(overall water bubble volume) in Fig. 5. VDF could amplify the contributions of the larger water bubbles with small number count in the dispersed phase, which was not shown in the PDF graph. According to the VDF, the specific bubbles with relatively larger diameters were found around 17–21 μm and 24–30 μm in W15 and W20 curves, respectively. The above results reveal that the destabilizing tendency increased with the increasing water content even though W20 still displayed one phase after the 14-day standing.

For grading the stability of different water additions, bubble diameter and SMD of W5, W10, W15, and W20 were measured and tabulated in Table 4. This result again indicated the instability of higher water fractions in emulsions which would flocculate, coalesce, and form a cream after an extended period of time which is supported by the aforementioned VDF graphs. From the micro-explosion point of view, Fu et al. [29] have reported that the micro-explosion strength has a maximum value around 40–60 vol.% of water and decreased with both lower and higher water content. This conclusion is supported by the fact that the storage energy of nucleation will be small and lead to weak micro-explosion when the water content is small; when water ratio is large, more water is needed to evaporate for keeping an oil membrane formation, which will lead to a smaller water portion left in dispersed bubble.

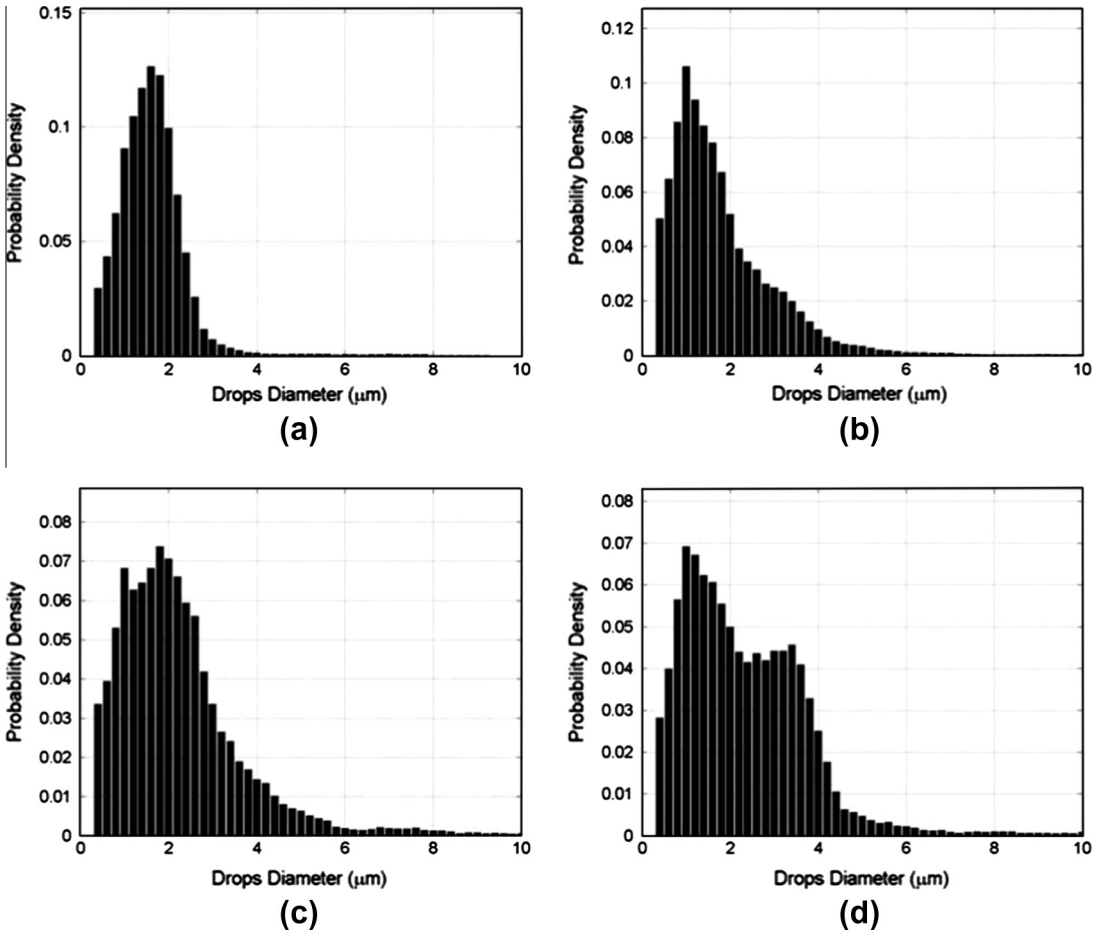

Fig. 4. Probability density functions of various W/O droplet diameters (a) W5, (b) W10, (c) W15, and (d) W20.

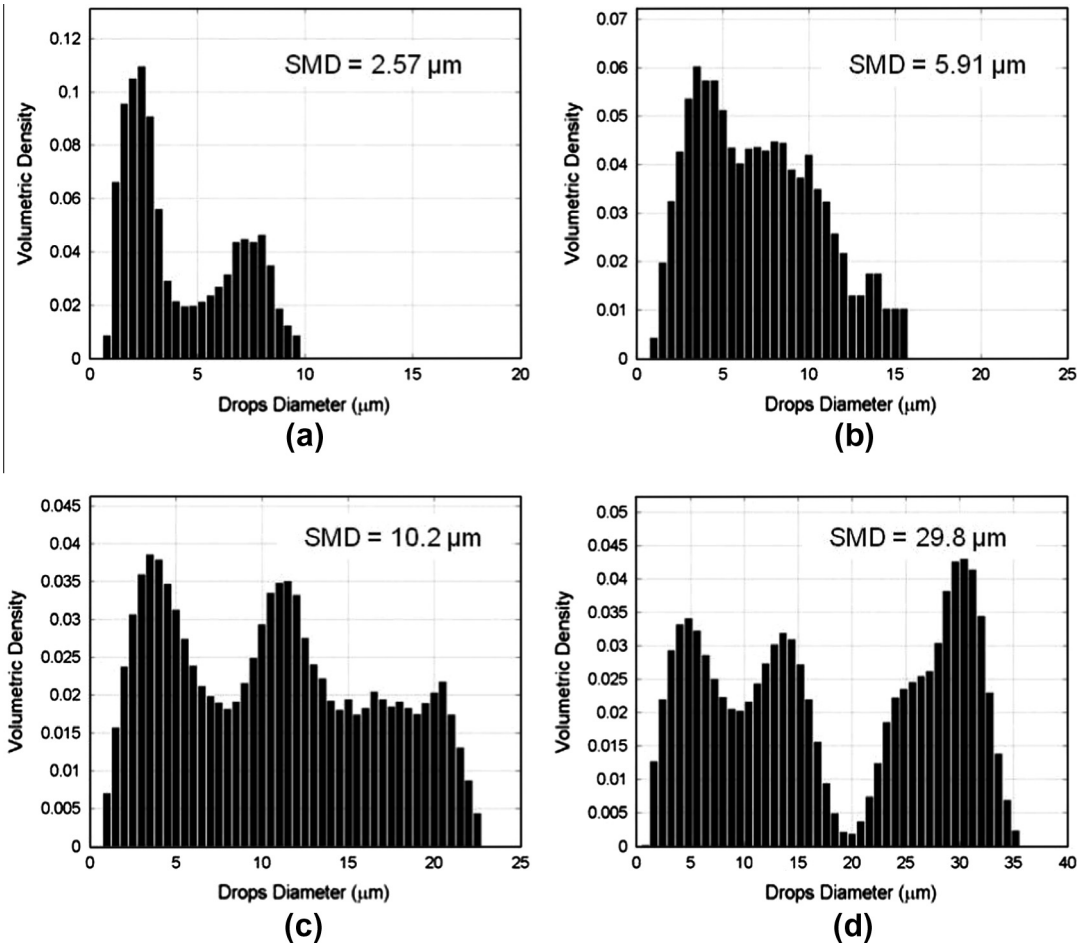

Fig. 5. Volumetric density fractions of various W/O droplet diameters (a) W5, (b) W10, (c) W15, and (d) W20.

Table 4
Bubble size of the emulsified diesel.

Fuel	W5	W10	W15	W20
d_{10} (μm)	1.5 ± 0.1	1.7 ± 0.1	2.1 ± 0.1	2.3 ± 0.1
d_{32} (μm)	2.6 ± 0.5	5.9 ± 1.2	10.2 ± 2.1	29.8 ± 4.8

In the current study, the generated emulsified fuel was stable, but also facilitated possible micro-explosion exploration in a burning spray. Consequently, W10 and W20 were chosen for the spray and combustion study because of their higher tendency and strength of micro-explosion while the storage time could still reach up to at least two weeks.

3.2. Spray liquid penetration

The evolution of the spray from individual shots for the tested fuels under ambient temperatures of 800 K and 1200 K are illustrated in Fig. 6. The images displayed are from the start of the injection with a time interval of 67 μs between consecutive images. Although all six spray plumes can be seen within the camera view, the laser beam was focused to illuminate only one plume, which explains the intensity difference observed among the plumes. The images were also "reversed" for better presentation of the downstream portion of the spray jet; in other words, the "black" region is the spray that was actually illuminated while the "white" region is actually dark in the original raw image. As expected, emulsified diesel presented longer liquid penetration compared to ULSD under low ambient temperatures because of the low volatility of the water, which is consistent with previous studies [21]. A thickened spray tip is observed for emulsified diesel at the beginning stage due to its higher viscosity and surface tension compared to ULSD, and consequently it's more resilient to primary breakup. It is thus speculated that the primary breakup occurred further downstream for the emulsified diesel under this condition. At an ambient temperature of 1200 K, emulsified fuel featured similar liquid penetration length as ULSD indicating that the ambient temperature impact outweighed the physical properties of the fuel. It is of particular interest to notice that two of the spray plumes of W10 were "fattened" at the early stages of the spray evolution; W20 also showed wider spray cone angle and shortened initial tip penetration in the first couple of snapshots but less apparent than those observed in W10. Because of the plume-to-plume variation, it is challenging to compare the spray pattern between ULSD and emulsified diesel on a statistical base. However, the initial fattened spray pattern does indicate more violent breakup which will be further discussed in the later section.

The quantitative measurement of the liquid penetration, based on the leading edge detection, is shown Fig. 7. We first recognize the error sources in this measurement technique. A threshold sensitivity test is first performed with the threshold ranging from 10% to 25% of the maximum pixel intensity and indicated that little sensitivity in intensity is found for the investigated range. Based on the visualization of the spray image, it is found that the major uncertainty arises from turbulent mixing at the leading edge after the combustion started. Although a narrow-band pass filter was

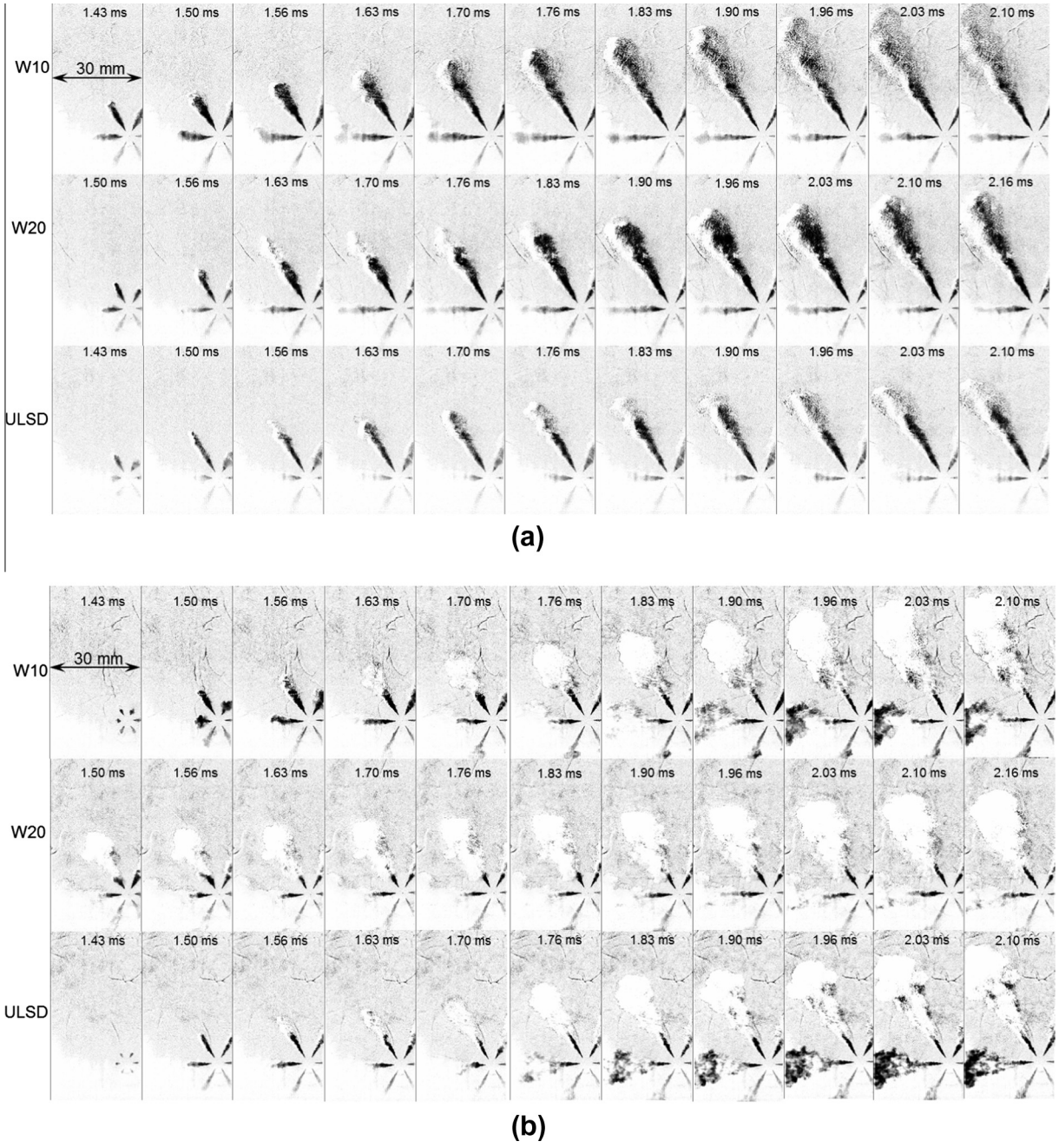

Fig. 6. Individual shots of liquid penetration with injection pressure of 70 MPa at ambient temperature of (a) 800 K and (b) 1200 K.

applied, strong soot incandescence may still contribute to the signal received by the camera as shown in Fig. 6b. Given the relative magnitude of the error sources, the liquid penetration calculation yielded a maximum uncertainty of up to 10% for the peak penetration length and an overall uncertainty of 5% on a shot to shot basis.

The fuel property and ambient temperature impact on liquid penetration is further justified in Fig. 7. At low ambient temperature of 800 K, water addition caused an initial longer penetration of the spray by around 40% compared to ULSD. A sudden steep drop in the curve, which coincided with the start of combustion timing, was observed for W10 and W20 indicating that the mixing-controlled flame stretched back towards the injector tip and swallowed the liquid jet spray. Both longer penetration and longer ignition delay will allow more air entrained in the lift-off which benefits the emission reduction. However, the initial long penetration has to be taken into account from the geometry point of view as wall wetting could potentially be caused under low temperature combustion mode, which may lead to high levels of hydrocarbon and carbon monoxide emissions as well as fuel/oil dilution, and consequently deteriorate engine performance. In comparison, the penetration under ambient temperature of 1200 K was significantly shorter and reached a quasi-steady state almost immediately after the onset of injection. The impact of the water addition was also much weakened due to the shorter ignition delay. Given the elevated ambient temperature conditions, the high evaporation rate and more violent breakup of the spray jet overwhelmed the impact of the physical properties of the fuel such as low volatility and higher surface tension.

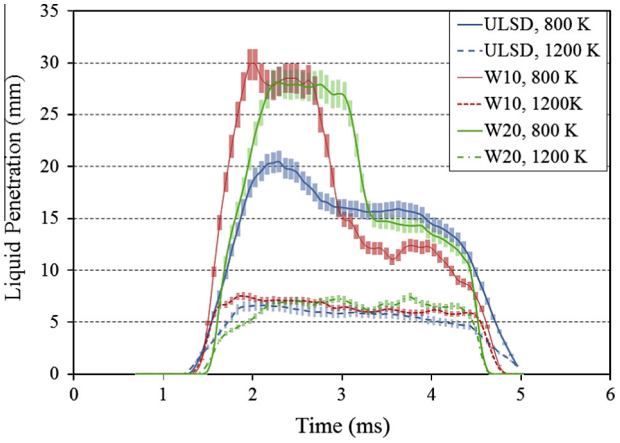

Fig. 7. Liquid penetration under various ambient temperatures.

3.3. Micro explosion

Fig. 8 illustrates three individual shots of the natural flame evolution near lift-off region for W10 at ambient temperature of 1200 K and injection presure of 70 MPa. As mentioned earlier, intentional overexposure was forced by using a relatively larger camera aperture which caused image saturation far downstream near the wall; however the liquid phase was also illuminated at the lift-off. Note that the quantitative flame luminosity analysis was carried out using another configuration where overexposure was carefully avoided. Abnormal droplet explosion along the lift-off was observed, just downstream of the injector tip at the beginning stage of combustion under high ambient temperature conditions. By further magnifying the image as shown in Fig. 9, the bright spots of similar or higher luminosity intensity than the lift-off, yet not as bright as the diffusion flame front, were seen scattered around the lift-off region. This droplet behavior has never been seen during the combustion of ULSD as illustrated in Fig. 10, indicating this could have resulted from micro-explosion because of the drastic boiling temperature difference between water and ULSD.

A previous study had reported "glowing spots" in the burning flame of emulsified fuel [22]. The observation in the current study, however, is different in several aspects. First, some of these scattered spots were not merely "glowing", but also visibly going through a violent disruption. As seen in the snapshots of Fig. 8a, the glowing spots near the lift-off of the left-most plume were still grouped together at 1.86 ms; a bumped part was raised from the spray core in the subsequent snapshot and it eventually burst into a number of tiny glowing spots at 2.33 ms; similar behavior is also observed in Fig. 8c. This spray behavior is very similar to the "puffing" observed in the single droplet micro-explosion measurement. The observation of such phenomena, as illustrated in the individual snapshot in Fig. 8, is on both a shot-to-shot and plume-to-plume basis, thus it is unreasonable to make any ensemble averaged analysis. Therefore, the authors took the approach that whenever such spray behavior was detected; at least five more runs would be executed under the same conditions to verify its consistency. Each condition will then be determined as either "observed" or "not observed" for such phenomena.

No apparent drops were detected from the Mie scattering image at the corresponding time as shown in Fig. 11, although a raised part from the liquid core was observed randomly. The absence of such drops in the spray images suggests that the glowing spots were most likely due to droplet combustion. According to the study of Watanabe and Okazaki [18], puffing and micro-explosion in the spray jet produces fine droplets with diameters in the order of several microns. While the visualization of such tiny droplets is difficult with the current imaging system in the author's lab, the presence of tiny liquid drops is speculated at the corresponding glowing spot locations which were under disruptive droplet combustion, and an imaging system with higher temporal and spatial resolution may capture them even in Mie scattering images. Also note that with the illumination of the flame luminosity, the puffing behavior of the emulsified spray at the lift-off is more easily detected than with the Mie scattering method. This is because although we used volumetric illumination, the light source was still just from one side of the spray; in other words, the puffing is difficult to be detected if it is overlapped, or even just partially overlapped with the jet core along the line-of-sight. Meanwhile, the luminosity from the flame itself provided multifaceted illumination, however, this intentional over-exposure approach will not work at low ambient temperature since the soot formation is suppressed which markedly lowered the flame natural luminosity.

The location of the scattered droplet combustion were also of interest since the glowing spots were reported in the diffusion flame while in the present study, these spots were found to be around lift-off at 1200 K indicating that it actually has an impact on the primary breakup at high ambient temperature. While previous works reported that micro-explosion enhanced the secondary breakup, it is shown that emulsified fuel has also an impact on the primary breakup at high ambient temperature. By decreasing the ambient temperature to 1000 K, such glowing spots, though much dimmer, were detected further downstream of the lift-off, which is similar to Raul's findings [22]. The location shift is due to the fact that the droplet combustion induced by micro-explosion was postponed under lower ambient temperature which is consistent with the findings in the single droplet test as the waiting time was found longer under lower ambient pressure conditions because it took longer time for the water phase to reach the superheat limit to form nucleation.

To further explore the injection pressure impact, four different injection pressures from 70 MPa to 130 MPa with an increment of 20 MPa were tested at an ambient temperature of 1200 K, and the duration of the observations are tabulated in Table 5. It should be mentioned that "not observed" only indicates no puffing or droplet combustion around the lift-off, but does not necessarily mean an absence of micro-explosion further downstream. It can be seen that with the increase the of the injection pressure, the duration of the occurrence of the puffing and glowing spots were reduced and eventually not observed for W10 at 130 MPa and W20 at 110 MPa and 130 MPa. The absence of such phenomena at elevated injection pressures is due to the competition of two characteristic time scales: the micro-explosion delay time and primary breakup time. High injection pressure induces more violent primary breakup due to the aerodynamic shear stress; once the primary breakup took place faster than the micro-explosion breakup, then micro-explosion will only impact the secondary breakup as considered in the traditional understanding. The increase of the water content may also lead to longer micro-explosion delay and decrease in the micro-explosion strength, which may explain the reason that such phenomena were not observed in W20 with injection pressure of 110 MPa compared with W10.

3.4. Integrated flame natural luminosity

The space integrated natural luminosity (SINL), as shown in Fig. 12, was calculated by integrating the pixel values over the entire image and averaged over five different runs. The flame natural luminosity consists of two parts; chemiluminescence and soot incandescence. The latter is much stronger than the former one within the camera responsible spectrum, thus it is reasonable to

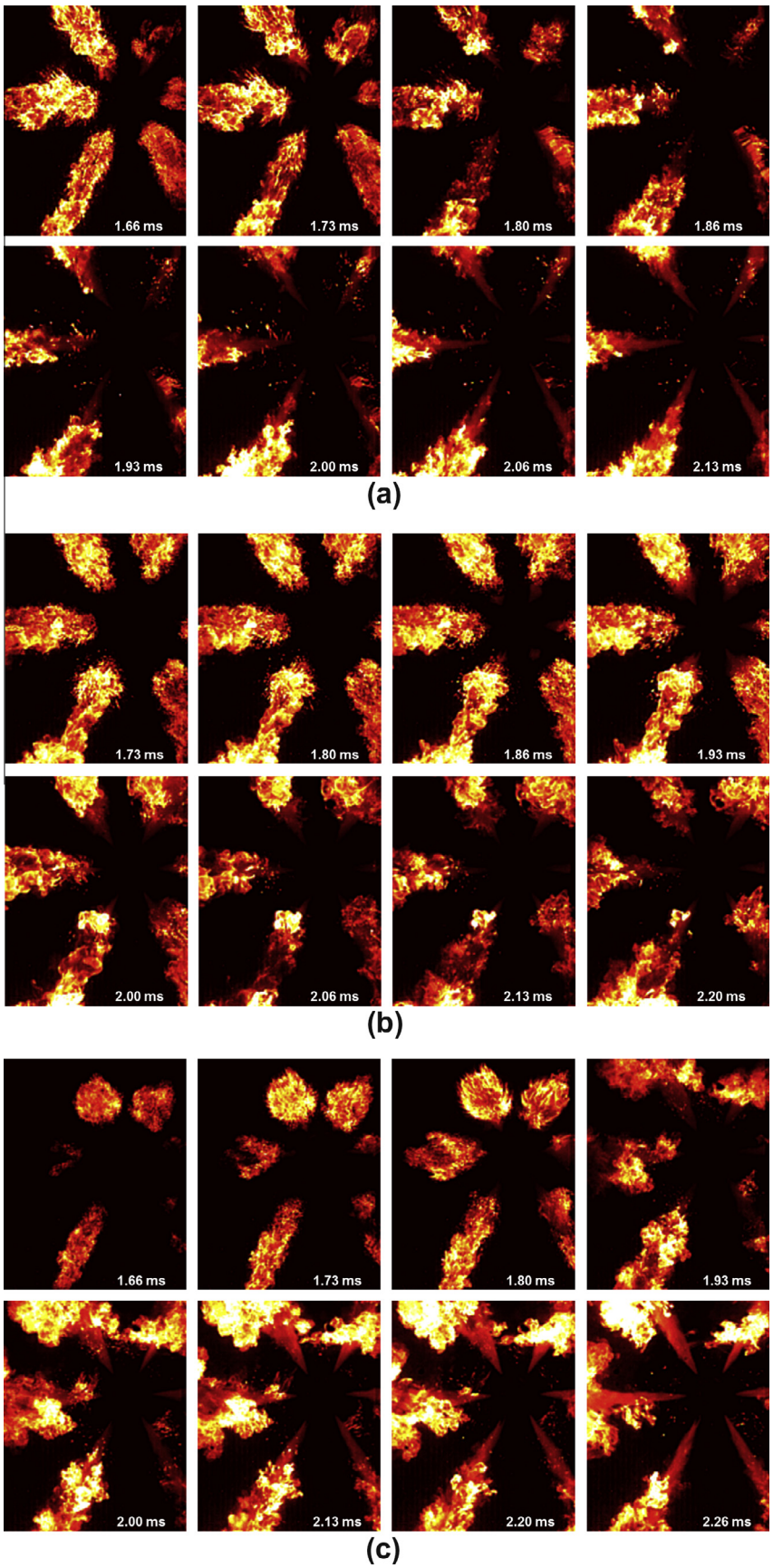

Fig. 8. Three individual shots of natural flame evolution near lift-off region for W10 at ambient temperature of 1200 K and P_{inj} = 70 MPa.

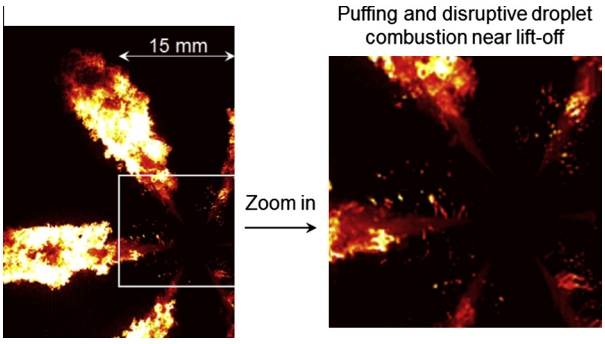

Fig. 9. Zoomed in near lift-off.

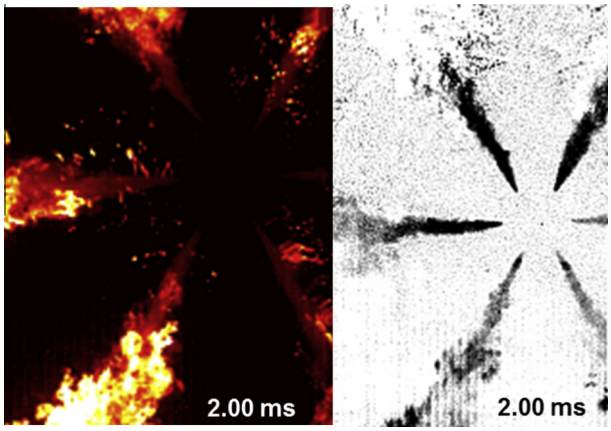

Fig. 11. Individual shots of flame natural luminosity and the Mie scattering image at the corresponding time.

argue that the soot luminosity can be well represented by the broadband luminosity, which is a good indication of the soot temperature and concentration. As expected, water addition led to lower soot luminosity especially under low ambient temperature conditions. The ignition, marked by the rise of the SINL, was remarkably retarded with the increase of the water content in the fuel at low ambient temperature, whereas negligible difference is noticed in the ignition delay at high ambient temperature. The results are consistent with the findings in the liquid penetration measurement. It is interesting to notice that the glowing spots observed around the lift-off at high ambient temperatures did not help the reduction of the soot luminosity at the start of combustion with W10. As water volumetric ratio increased to 20%, the initial soot luminosity is lower as featured by the less steep rise of the slope, indicating that the cooling impact of the latent heat of water may have a larger contribution to the soot reduction.

To better quantify the natural luminosity characteristics of the entire combustion duration, time integrated natural luminosity (TINL) was calculated by further integrating the SINL with time. TINL is an indication of the soot temperature and concentration over the entire combustion cycle. Fig. 13 illustrates the TINL for tested fuels at various ambient temperatures. The addition of the water lowered the TINL due to better atomization characteristics of the fuel as well as the evaporative cooling of water, which effectively suppressed the soot formation. It is found that the reduction in TINL magnitude between 10% and 20% water was typically larger than that between 0% and 10%, most likely due to the much retarded ignition delay and more homogeneous mixture prepared before the onset of combustion. The high water content, however, has more tendencies to be unstable as aforementioned. In this regard, the emission-stability trade-off will be an interesting study in the future for the application of emulsified fuel.

Table 5
Duration of the observed disruptive droplet combustion at ambient temperature of 1200 K.

	Injection pressure			
	70 MPa	90 MPa	110 MPa	130 MPa
D100	×	×	×	×
W10	1.66 ± 0.6–3.33 ± 1.3 ms	1.86 ± 0.6–2.26 ± 0.6 ms	1.86 ± 0.4–2.00 ± 0.4 ms	×
W20	1.80 ± 0.6–3.33 ± 1.3 ms	1.73 ± 0.6–2.93 ± 0.6 ms	×	×

× – Not observed.

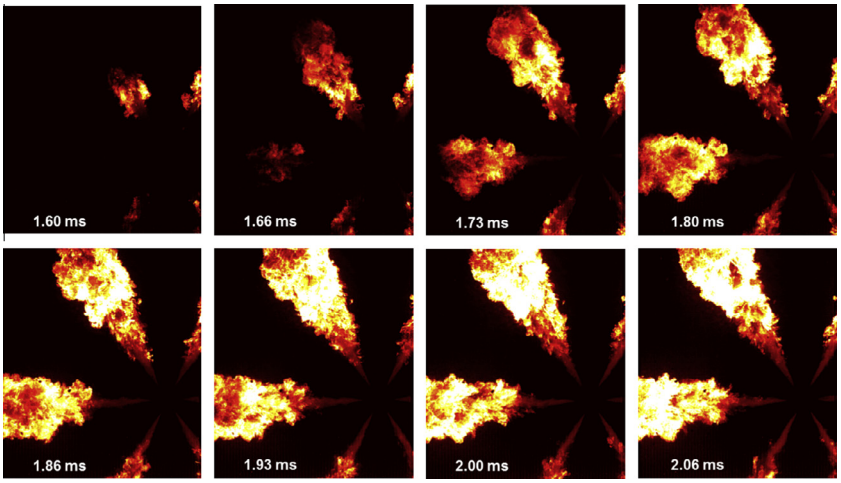

Fig. 10. Natural flame evolution at lift-off for ULSD at ambient temperature of 1200 K and P_{inj} = 70 MPa.

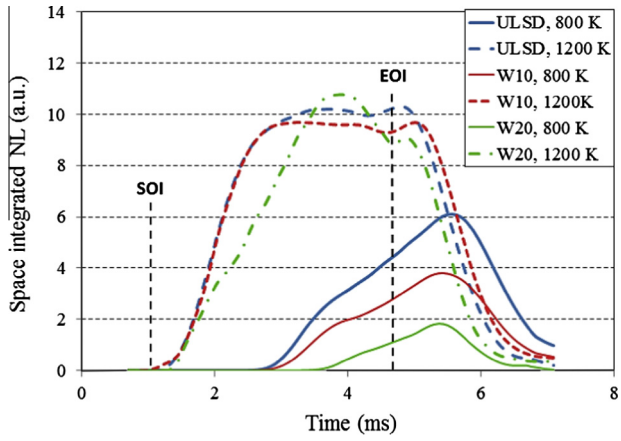

Fig. 12. SINL at various ambient temperatures.

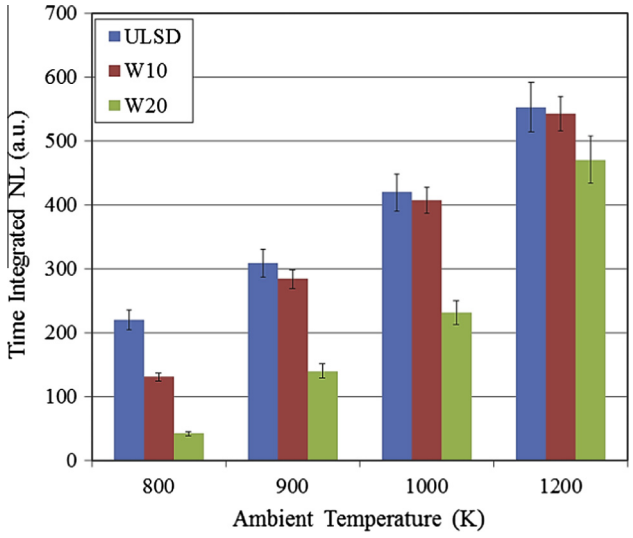

Fig. 13. TINL at various ambient temperatures.

4. Conclusion

The spray and combustion characteristics of water emulsified fuel with different blending ratio were experimentally investigated in a constant volume combustion chamber with different injection pressures and under various ambient temperatures. Following conclusions can be reached based on this study:

1. An HLB value of five is relatively the most suitable surfactant composition to the diesel/water interfacial condition. Volumetric density of the water phase bubble size calculated from micro images revealed that the destabilizing tendency increased with the increasing water content even though W20 still presented a single phase after a 14-day standing.
2. Emulsified diesel manifested longer liquid penetration and longer ignition delay under low ambient temperatures due to the lower volatility and higher viscosity of the water. At high ambient temperature, the physical properties of the fuel are weakened; the spread spray cone angles indicated violent breakup events taking place upstream of the spray jet.
3. Applying the intentional over-exposure approach, the liquid phase of the spray could be illuminated by the soot incandescence in the broadband luminosity imaging. Glowing spots resulting from disruptive droplet combustion were consistently observed under certain conditions which have resulted from micro-explosion. It is demonstrated that emulsified fuel could also affect the primary breakup instead of the secondary breakup under low injection pressure and high ambient temperature conditions.
4. Low injection pressure and higher ambient temperature favor the occurrence of puffing and disruptive droplet combustion at the lift-off as a competition of the micro explosion delay time and primary breakup time. Once the primary breakup timescale is shorter, the micro-explosion may only facilitate the secondary atomization and the glowing spots at the lift-off will no longer be observed.

Acknowledgement

This material is based upon work supported by the National Science Foundation under Grant No. CBET-1236786. Any opinions, findings, and conclusions or recommendations expressed in this publication are those of the author(s) and do not necessarily reflect the views of the National Science Foundation. This work was also supported in part by the Special Program for International Science and Technology Cooperation Projects of Zhejiang Province under Grant No. 2012C24006.

References

[1] Valdmanis E, Wurlfhorst DE. Effects of emulsified fuels and water induction on diesel combustion. SAE 700736; 1970.
[2] Song KH, Lee YJ. Effects of emulsified fuels on soot evolution in an optically-accessible DI diesel engine. SAE, 2000-01-2794.
[3] Musculus PPB, Dec JE, Tree DR, Daly D, Langer D, Ryam TW, et al. Effects of water fuel emulsions on spray and combustion processes in a heavy-duty DI diesel engine. SAE 2003-01-3146; 2003.
[4] Anna L, Magnus S, Savo G, Ingemar D. Reduction of soot emissions from a direct injection diesel engine using water-in-diesel emulsions and micro emulsion fuels. SAE 2007-01-1076; 2007.
[5] Kadota T, Yamasaki H. Recent advances in the combustion of water fuel emulsion. Prog Energy Combust Sci 2002;28:385–404.
[6] Lin CY, Lin SA. Effects of emulsification variables on fuel properties of two- and three-phase biodiesel emulsions. Fuel 2007;86:210–7.
[7] Botero ML, Huang Y, Zhu DL, Molina A, Law CK. Synergistic combustion of droplets of ethanol diesel and biodiesel mixtures. Fuel 2012;94:342–7.
[8] Mura E, Massoli P, Josset C, Loubar K, Bellettre J. Study of the micro-explosion temperature of water in oil emulsion droplets during the Leidenfrost effect. Exp Therm Fluids Sci 2012;43:63–70.
[9] Gong JS, Fu WB. A study on the effect of more volatile fuel on evaporation and ignition for emulsified oil. Fuel 2001;80:437–45.
[10] Tsue T, Kadota T, Segawa D. Statistical analysis on onset of microexplosion for an emulsion droplet. Proc Combust Inst 1996;24:1629–35.
[11] Tsue T, Yamasaki H, Kadota T, Segawa D, Kono M. Effect of gravity on onset of microexplosion for an oil-in-water emulsion droplet. Proc Combust Inst 1998;26:2587–93.
[12] Kadota T, Tanaka H, Segawa D, Nakaya S, Yamasaki H. Microexplosion of an emulsion droplet during Leidenfrost burning. Proc Combust Inst 2007;31:2125–31.
[13] Watanabe H, Harada T, Matsushita Y, Aoki H, Miura T. The characteristics of puffing of the carbonated emulsified fuel. Int J Heat Mass Transfer 2009;52:3676–84.
[14] Watanabe H, Suzuki Y, Harada T, Matsushita Y, Aoki H, Miura T. An experimental investigation of the breakup characteristics of secondary atomization of emulsified fuel droplet. Energy 2010;35:806–13.
[15] Morozumi Y, Saito Y. Effect of physical properties on microexplosion occurrence in water-in-oil emulsion droplets. Energy Fuels 2010;24:1854–9.
[16] Mattiello M, Cosmai L, Pistone L. Experiment evidence for microexplosions in water/fuel oil emulsion flames inferred by laser light scattering. Symp Combust 1992;24:1573–8.
[17] Wu DY, Sheng HZ, Zhang HC, Wei XL. Study on micro-explosions procedure of diesel/water/methanol emulsions droplet. J Xi'an Jiaotong Univ 2007;41:772–5.
[18] Watanabe H, Okazaki K. Visualization of secondary atomization in emulsified-fuel spray flow by shadow imaging. Proc Combust Inst 2013;34:1651–8.
[19] Mizutani Y, Fuchihata M, Matsuoka Y, Muraoka M. Observation of micro-explosion in spray flames of light oil-water emulsions. Trans Jpn Soc Mech Eng B 2000;66:1544–9.

[20] Fuchihata M, Ida T, Mizutani Y. Observation of microexplosions in spray flames of light oil-water emulsions (2nd report, influence of temporal and spatial resolution in high speed videography). Trans Jpn Soc Mech Eng B 2003;69:1503–8.
[21] Takeda S, Fuchihata M, Ida T. Observation of microexplosions in spray flames of light oil-water emulsions (3rd report, influence of the diameter of dispersed water droplets on the spray flame structure). Trans Jpn Soc Mech Eng B 2008;74:1649–53.
[22] Raul O, Anna L, Magnus N, Sven A, Ingemar D. Optical studies of spray development and combustion of water-in-diesel emulsion and micro emulsion fuels. Fuel 2010;89:122–32.
[23] Park JW, Huh KY, Park KH. Experimental study on the combustion characteristics of emulsified diesel in a rapid compression and expansion machine. PI Mech Eng D – J Aut 2000;214:579–86.
[24] Lin YS, Lin HP. Study on the spray characteristics of methyl esters from waste cooking oil at elevated temperature. Renew Energy 2010;35:1900–7.
[25] Sheng HZ, Chen L, Zhang ZP, Wu CK. The droplet group microexplosion in water-in-oil emulsion sprays and their effects on diesel engine combustion. Symp Combust 1994;25:175–81.
[26] Liu HF, Lee CF, Huo M, Yao MF. Comparison of ethanol and butanol as additives in soybean biodiesel using a constant volume combustion chamber. Energy Fuels 2011;25:1837–46.
[27] Liu HF, Bi XJ, Huo M, Lee CF, Yao MF. Soot emissions of various oxygenated biofuels in conventional diesel combustion and low-temperature combustion conditions. Energy Fuels 2012;26:1900–11.
[28] Liu HF, Lee CF, Huo M, Yao MF. Combustion characteristics and soot distributions of neat butanol and neat soybean biodiesel. Energy Fuels 2011;25:3192–203.
[29] Fu WB, Hou LY, Wang L, Ma FH. A unified model for the micro-explosion of emulsified droplets of oil and water. Fuel Proc Technol 2002;79:107–19.